

Stellar Positioning System (Part I): Applying Ancient Theory to a Modern World

Julie J. Parish*, Allen S. Parish†, Michael Swanzky‡
Drew Woodbury§, Daniele Mortari¶ and John L. Junkins||
Texas A&M University, College Station, Texas 77843-3141

Two different theoretical approaches to the position determination problem are presented, one matrix-based and the other vector-based. Both approaches are designed for implementation in an autonomous Stellar Positioning System (SPS) that uses the following measurement sources: an astronomical camera, a clock, and a set of two inclinometers. Before presenting each of the algorithms, the reference frames utilized are defined. The two position estimation techniques are then individually presented, followed by a discussion of real-world gravity and geometry model refinements.

I. Introduction

The stars have been used for position determination for centuries, but inaccuracies in star catalogs and clocks introduced error in early navigation.¹ Today, more precise clocks and reliable star catalogs exist, but celestial positioning techniques have been replaced by GPS technology. GPS is able to locate a position on Earth to sub-meter precision; however, its capabilities are limited by the necessary constellation of satellites used to accurately determine position. Consequently, GPS cannot be used on the moon or other planets without establishing a similar constellation beforehand. Setting up satellite constellations for simple exploration is too costly and an alternative positioning system is needed. The Stellar Position System (SPS) offers a modern version of the ancient celestial navigation tools—an autonomous stellar positioning algorithm.

In this paper, both a matrix-based method and vector-based method for solving the position determination problem are presented. Though the SPS is intended to be deployed in an extraterrestrial environment, the initial development is presented with respect to an Earth model. The SPS reference frames and measurement sources will first be defined and then subsequently employed in the discussion of each algorithm. Refinements to the initial Earth model, assumed to be spherical, will then be described. Finally, a brief overview of implementation obstacles is provided, with a full discussion of hardware and data processing solutions available in Stellar Positioning System (Part II).²

II. Reference Frames

Several reference frames are employed in the position determination algorithms. The first of these is the inertial reference frame, denoted by the subscript I , also called the Earth Centered Inertial (ECI) frame. This frame is particularly important because it is assumed that the star catalogs provide the reference vectors for the stars in this frame. Note that the X-axis of this frame is aligned with the vernal equinox, or the ascending node of the geocentric elliptic, and the XY-plane is coplanar with the equatorial plan. The Greenwich reference frame, $\{G\}$, also called the Earth-Centered Earth-Fixed (ECEF) frame, describes the location of the Greenwich, or Prime, Meridian that corresponds to a longitude of 0° . The orientation of

*Ph.D. Student, Department of Aerospace Engineering, TAMU-3141, Student Member AIAA.

†M.S. Student, Department of Computer Engineering, TAMU-3112.

‡M.S. Student, Department of Aerospace Engineering, TAMU-3141.

§Ph.D. Student, Department of Aerospace Engineering, TAMU-3141, Student Member AIAA.

¶Associate Professor, Department of Aerospace Engineering, TAMU-3141, Member AIAA.

||Distinguished Professor, George Eppright Chair, Department of Aerospace Engineering, TAMU-3141, Fellow AIAA.

this frame relative to the inertial frame (figure 1) is described by the direction cosine matrix (DCM) $\mathbf{R}_{G/I}$, which is primarily a function of time, $\Psi(t)$. A simple approximation of this angle would be $\Psi = \omega_e t$, where ω_e is the Earth rotation rate. A more rigorous discussion of the direction cosine matrix (DCM) between the Greenwich and inertial frames, $\mathbf{R}_{G/I}$, is presented in Section V.B.

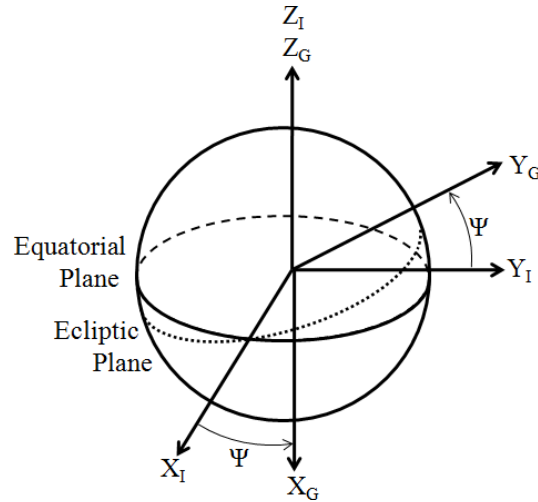


Figure 1. Inertial $\{I\}$ and Greenwich $\{G\}$ Frames

The orientation of the local frame, $\{L\}$, is described relative to the Greenwich frame via latitude, ϕ , and longitude, λ angles. These angles are used to construct the DCM between the Local and Greenwich frames, $\mathbf{R}_{L/G}$. The X_L and Y_L axes of the local frame are aligned with the standard compass directions South and East, respectively, while the Z_L axis is parallel to the zenith direction. The system lies in the plane tangential to the local position but may not be aligned with the local frame. A rotation about the Z_L axis by a compass angle, θ accounts for the heading angle in the local frame to compass frame, $\{C\}$, direction cosine matrix, $\mathbf{R}_{C/L}$. Figure 2 shows the relationship between the three frames.

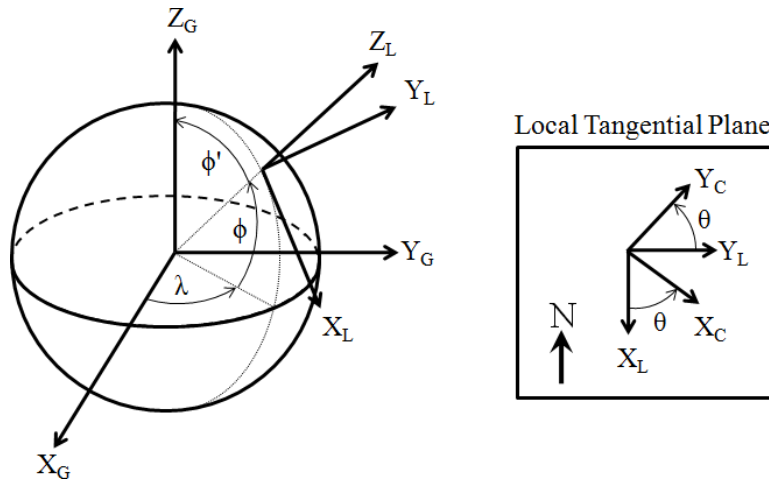


Figure 2. Greenwich $\{G\}$, Local $\{L\}$, and Compass $\{C\}$ Frames

The final reference frame is the body frame, $\{B\}$, which correlates to the image plane of the camera. The angle measurements from the inclinometers are used to find the attitude transformation from the compass to the body frame, $\mathbf{R}_{B/C}$, as described in detail in Section C for the matrix method. Together, this set of frames and the DCMs relating the frames are used to estimate the position and/or attitude of the system through the matrix and/or vector methods.

III. Measurement Sources

In implementation, both estimation approaches use the same measurement sources: an astronomical camera, a clock, and a set of two inclinometers. The camera, coupled with both a centroiding algorithm and the pyramid star identification algorithm,³ is used as a star tracker. The measurements obtained here include the vector locations, in both the Earth Centered Inertial (ECI) reference frame and the camera (“body”) reference frame, of stars observed in the camera field of view (FOV). The inclinometer measurements provide information used to calculate the direction of the gravity gradient. This measurement is akin to the location of the horizon in early celestial navigation techniques. The time measurement is converted to an angle and used to find the orientation of the Earth relative to an inertial frame. A basic flow chart relating the measurements to the position determination algorithms of the SPS is presented in figure 3.

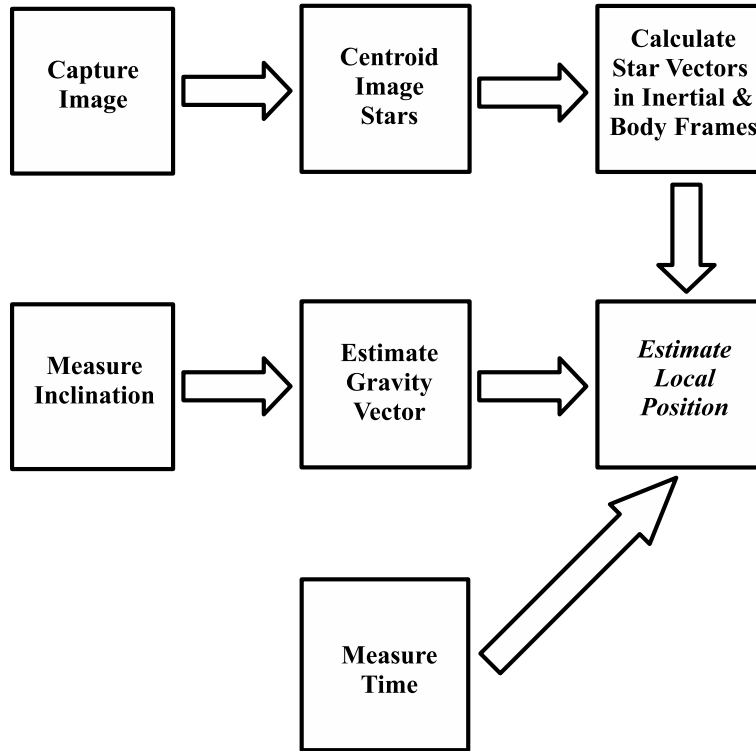


Figure 3. Basic SPS Local Position Determination Algorithm.

IV. Position Determination Algorithms

The theory behind the position determination algorithms is founded in fairly straightforward geometry, coordinate transformation, and linear algebra concepts. This section discusses these concepts for a spherical model of the Earth.

A. Matrix Method

The matrix method for estimating the local position of the system exploits the structure of the rotation matrix relating the Greenwich and Local reference frames.

$$\mathbf{R}_{L/G} = \mathbf{R} = \begin{bmatrix} \cos \phi' \cos \lambda & \cos \phi' \sin \lambda & -\sin \phi' \\ -\sin \lambda & \cos \lambda & 0 \\ \sin \phi' \cos \lambda & \sin \phi' \sin \lambda & \cos \phi' \end{bmatrix} \quad (1)$$

Here, λ is the longitude, ϕ is the latitude, and $\phi' = 90^\circ - \phi$ is the complement of the latitude. The following trigonometric properties can be utilized with the matrix entries.

$$\begin{aligned}\lambda &= \arctan\left(\frac{\mathbf{R}(3,2)}{\mathbf{R}(3,1)}\right) \\ \phi' &= \arcsin\left(\frac{\mathbf{R}(3,2)}{\sin \lambda}\right) = \arcsin\left(\frac{\mathbf{R}(3,1)}{\cos \lambda}\right) \\ \phi &= 90^\circ - \phi'\end{aligned}\tag{2}$$

The remaining question is how to find this matrix from the available measurements. The DCMs $\mathbf{R}_{B/I}$ and $\mathbf{R}_{I/G}$ can be computed using camera images²⁻⁴ and time measurements (see Sections II, V.B), respectively. The product of these matrices composes the left hand side of the primary equation to be solved.

$$\mathbf{R}_{B/I}\mathbf{R}_{I/G} = \mathbf{R}_{B/C}\mathbf{R}_{C/L}\mathbf{R}_{L/G}\tag{3}$$

On the right hand side of the equation, $\mathbf{R}_{B/C}$ can also be calculated using inclinometer measurements (see Section IV.C), and can be moved to the left hand side. The remaining term in the equation for which one must account is the DCM from the compass to local frame, $\mathbf{R}_{C/L}$. Because our matrix equation is of dimension three and there are thus far only two unknowns presented, the compass direction, θ , can be defined as the third unknown. Note that when this unknown is introduced into Eq. (3), the trigonometric properties of Eq. (1) are still valid for the product $\mathbf{R}_{C/L}\mathbf{R}_{L/G}$.

$$\mathbf{R}_{C/L}\mathbf{R}_{L/G} = \begin{bmatrix} C_\theta & S_\theta & 0 \\ -S_\theta & C_\theta & 0 \\ 0 & 0 & 1 \end{bmatrix} \begin{bmatrix} C_{\phi'}C_\lambda & C_{\phi'}S_\lambda & -S_{\phi'} \\ -S_\lambda & C_\lambda & 0 \\ S_{\phi'}C_\lambda & S_{\phi'}S_\lambda & C_{\phi'} \end{bmatrix}\tag{4a}$$

$$\mathbf{R}_{C/L}\mathbf{R}_{L/G} = \begin{bmatrix} C_\theta C_{\phi'} C_\lambda - S_\theta S_\lambda & C_\theta C_{\phi'} S_\lambda + S_\theta C_\lambda & -C_\theta S_{\phi'} \\ -S_\theta C_{\phi'} C_\lambda - C_\theta S_\lambda & -S_\theta C_{\phi'} S_\lambda + C_\theta C_\lambda & S_\theta S_{\phi'} \\ S_{\phi'} C_\lambda & S_{\phi'} S_\lambda & C_{\phi'} \end{bmatrix}\tag{4b}$$

Here, $C_x \equiv \cos x$ and $S_x \equiv \sin x$. Using the aforementioned trigonometric equations from Eq. (1) and the calculated elements of the matrix of the left hand side of the equation $\mathbf{R}_{B/C}^T \mathbf{R}_{B/I} \mathbf{R}_{I/G} = \mathbf{R}_{C/L} \mathbf{R}_{L/G}$, the position latitude and longitude can be determined. Note that the latitude is the geocentric latitude. Conversion to geodetic latitude will be further discussed in Section V.A. Also, if one were also interested in the the compass direction, θ , this could be derived from the matrix components in a similar manner.

B. Vector Method

The vector method explicitly mirrors the global positioning algorithms of old. Before the advent of GPS, navigators used the angles between the horizon and stars, the sun, etc., to calculate position. Here, instead of the horizon, the gravity vector, \mathbf{g} , is used as a local reference. It is assumed that the local gravity vector is orthogonal to the local horizontal plane (“horizon”), as shown in figure 4.

Using a geocentric spherical Earth model, the gravity vector points in the opposite direction of the local position vector, a function of the latitude and longitude.

$$\mathbf{g} = -\boldsymbol{\ell} = \begin{bmatrix} \cos \phi \cos \lambda \\ \cos \phi \sin \lambda \\ \sin \phi \end{bmatrix}\tag{5}$$

Here, ϕ and λ are the geocentric latitude and longitude, respectively. Let β_i describe the angle between the direction of the star \mathbf{r}_i and gravity \mathbf{g} . The elevation angle measured by inclinometers, α_i , can be related to β_i with $\alpha_i = \beta_i - \pi/2$. Written in the body reference frame, the star reference vector and gravity vector are related to β_i through the inner product.

$${}^B \mathbf{r}_i^T \mathbf{g} = \cos \beta_i\tag{6}$$

Because angles are independent of reference frames, this equation can also be written in the Greenwich reference frame.

$$-{}^G \mathbf{r}_i^T \boldsymbol{\ell} = \cos \beta_i\tag{7}$$

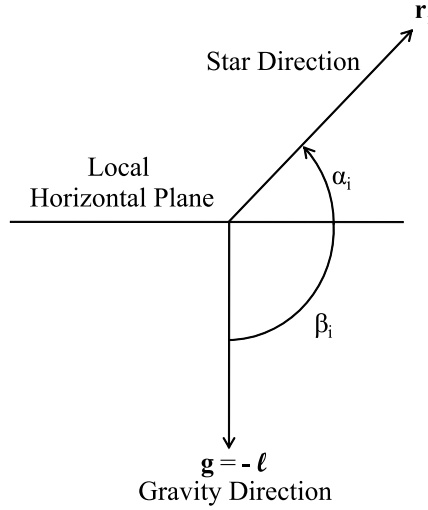


Figure 4. Gravity replaces the horizon as the local reference measurement.

Together, Eqs. (6) and (7) allow one to write the following identity for each observed star.

$${}^G\mathbf{r}_i^T \boldsymbol{\ell} = -{}^B\mathbf{r}_i^T \mathbf{g} \quad (8)$$

These n equations can also be written in matrix form.

$$\mathbf{A}_G \boldsymbol{\ell} = \begin{bmatrix} {}^G\mathbf{r}_1^T \\ {}^G\mathbf{r}_2^T \\ \vdots \\ {}^G\mathbf{r}_n^T \end{bmatrix} \boldsymbol{\ell} = - \begin{bmatrix} {}^B\mathbf{r}_1^T \\ {}^B\mathbf{r}_2^T \\ \vdots \\ {}^B\mathbf{r}_n^T \end{bmatrix} \mathbf{g} = -\mathbf{A}_B \mathbf{g} \quad (9)$$

The least squares solution for the local position estimate is then the following.

$$\boldsymbol{\ell} = -(\mathbf{A}_G^T \mathbf{A}_G)^{-1} \mathbf{A}_G^T \mathbf{A}_B \mathbf{g} = \begin{Bmatrix} \cos \phi \cos \lambda \\ \cos \phi \sin \lambda \\ \sin \phi \end{Bmatrix} \quad (10)$$

where ϕ and λ are the latitude and longitude, respectively.

The simplicity of this straightforward method recommends it as the least error-prone and most easily implemented solution for position determination.

C. Cones Intersection Method

The cones intersection method is used to find the gravity vector in the vector method and the matrix $\mathbf{R}_{B/C}$ in the matrix method. Here, the two system inclinometers are assumed to be aligned with the \mathbf{X}_B and \mathbf{Y}_B axes of the body frame, with the optical axis of the camera aligned with the \mathbf{Z}_B axis, as shown in figure 5. In the case that the inclinometers are not aligned to these axes, the location of the inclinometers in the body frame would have to be calculated, as earlier discussed. The \mathbf{Z}_C axis $\{C\}$ frame, or the compass frame, is collinear with the gravity direction: $\mathbf{g} = -|g|\mathbf{Z}_C$.

The angular measurements of the \mathbf{X}_B and \mathbf{Y}_B inclinometers from the horizontal state are ξ and η respectively. As shown in above, these angles are measured independently by each inclinometer. The geometric solution for the the zenith direction, \mathbf{Z}_C and the attitude matrix between the two frames, $\mathbf{R}_{B/C}$, represent the intersection of two cones defined by the angular measurements ξ and η . The cones intersect at two points, one of which corresponds to the zenith axis, \mathbf{Z}_C . Let the components of the vector $\mathbf{Z}_C = [x, y, z]$ in the body (camera) frame. Figure 6 shows the two cones defined by ξ and η .

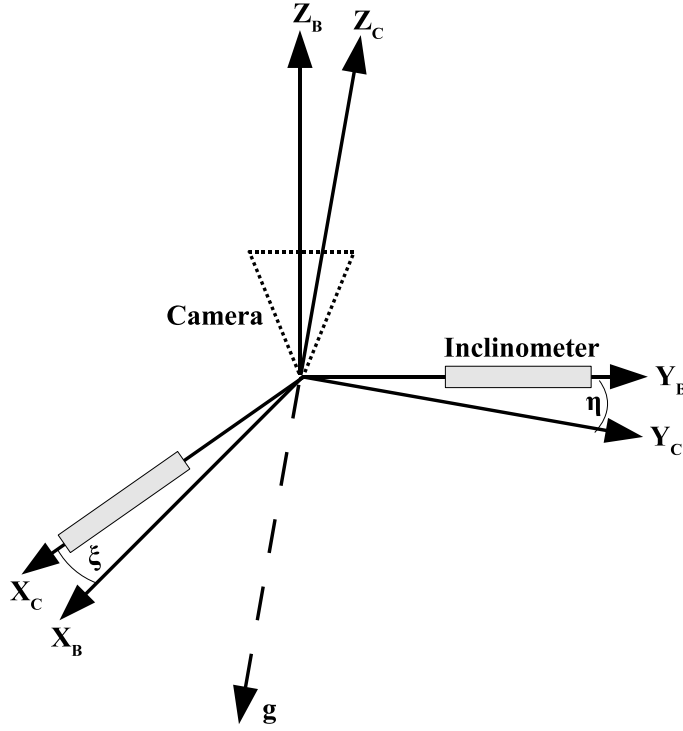


Figure 5. System Body Frame Alignment

To begin, consider the equation of a circle of radius r in \mathcal{R}^3 .

$$x^2 + y^2 + z^2 = r^2 \quad (11)$$

Now, consider the case when the angle ξ is the only unknown. A known, given angle η , can be paired with the angle ξ , ranging from $0 \rightarrow 2\pi$ radians to trace a circle with the zenith axis, \mathbf{Z}_C . Simple geometry yields the radius of the circle: $r = \cos \eta$. Alternatively, it is known that the circle lies entirely on the plane where $x = \sin \eta$. This value can be substituted in Eq. 11 to give the following relationship.

$$y^2 + z^2 = r^2 = 1 - \sin^2 \eta \quad (12)$$

It should be clear that this development for an unknown angle η could easily be translated to the case where ξ is known and η is varied from $0 \rightarrow 2\pi$ radians. In this case, the circle lies on the plane where $y = \sin \xi$, and the resulting equation for the circle traced by the optical axis is the following.

$$x^2 + z^2 = r^2 = 1 - \sin^2 \xi \quad (13)$$

Naturally, both points of conic intersection will satisfy $x = \sin \eta$ and $y = \sin \xi$. All that remains is to solve for z . Substitution of the x and y constraints into Eq. 11 results in the following possible solutions for z .

$$z = \pm \sqrt{1 - \sin^2 \eta - \sin^2 \xi} \quad (14)$$

The combination of the constraints imposed by the inclinometer sensor and the physical practicalities of sky-viewing eliminate the possibility of a negative z solution. Furthermore, a negative z value would indicate a zenith axis direction below the horizon. The optical axis vector is therefore

$$\mathbf{Z}_C = [\sin \eta \quad \sin \xi \quad \sqrt{1 - \sin^2 \eta - \sin^2 \xi}] \quad (15)$$

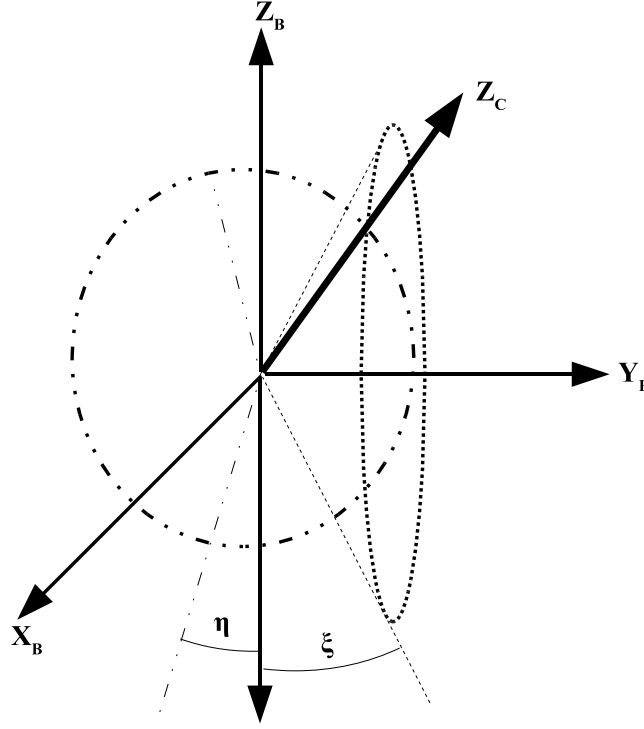


Figure 6. The geometric solution for Z_C

This solution corresponds to the negative of the direction of the gravity vector. The axes \mathbf{X}_C and \mathbf{Y}_C must be determined in order to solve for the entire attitude matrix. Because $\mathbf{R}_{B/C}$ is orthonormal, the following equations must also hold true.

$$\begin{aligned} \mathbf{Y}_C \cdot \mathbf{Z}_C &= 0 & \mathbf{X}_C \cdot \mathbf{Z}_C &= 0 & \mathbf{Y}_C \cdot \mathbf{X}_C &= 0 \\ \mathbf{Y}_C \times \mathbf{Z}_C &= \mathbf{X}_C & \mathbf{X}_C \cdot \mathbf{X}_C &= 1 & \mathbf{Y}_C \cdot \mathbf{Y}_C &= 1 \end{aligned} \quad (16)$$

One solution path begins by relating terms of the vector expression $\mathbf{Y}_C \times \mathbf{Z}_C = \mathbf{X}_C$. The solutions for the vector components $Y_C(3)$ and $Y_C(1)$ are given by the following expressions.

$$\mathbf{Y}_C(3) = \frac{\cos \xi \sqrt{1 - \sin^2 \eta - \sin^2 \xi} - \cos \eta}{\sin \xi} \quad (17)$$

$$\mathbf{Y}_C(1) = -\frac{\cos \xi \sin \xi + y'(3) \sqrt{1 - \sin^2 \eta - \sin^2 \xi}}{\sin \eta} \quad (18)$$

Recall that the inclinometers move in the $\{x - z\}$ or $\{y - z\}$ compass frame planes only, so the values $\mathbf{X}_C(1) = \cos \xi$ and $\mathbf{Y}_C(2) = \cos \eta$ are known. Finally, because \mathbf{Y}_C should have unit length, the solution for the vector is the following.

$$\mathbf{Y}_C = \frac{\mathbf{Y}_C}{\|\mathbf{Y}_C\|} \quad (19)$$

To complete the solution, \mathbf{X}_C is known to be the cross-product of \mathbf{Y}_C and \mathbf{Z}_C , both of which are now fully defined. The attitude of the camera body with respect to the local reference frame is then the following.

$$\mathbf{R}_{B/C} = [\mathbf{X}_C \quad \mathbf{Y}_C \quad \mathbf{Z}_C] \quad (20)$$

Due to the trigonometric terms in the solution path currently presented, singularities exist when either angle becomes 0° or 90° . The singularity that occurs when one angle becomes 0° is easily handled as a single Euler axis rotation about the \mathbf{X}_B or \mathbf{Y}_B axis, as appropriate. As for the 90° case, the system is not intended for observations near the horizon which eliminates any concern for this obstacle.

V. Model Refinements

In the development of the position determination algorithm for the SPS, some implicit assumptions are made. First, the gravity vector is assumed to point to the center of a spherical Earth. Second, again using an ideal spherical Earth, the $\mathbf{R}_{G/I}$ attitude transformation is assumed to be a single simple rotation with an angle that is an explicit function of time. The accuracy of these assumptions must be further investigated, and corrections to them must be applied as necessary.

A. Earth Model

Although the reference frame drawings depict the Earth as a sphere, these representations are simplifications. The rotation of the Earth actually causes a more ellipsoidal shape. As a result, the simple geometry assumed in the latitude description of the $\mathbf{R}_{G/I}$ attitude transformation matrix is no longer valid. Rather, some additional modeling of the Earth’s geometry—and gravity field—is necessary to relate the frames to actual local measurements. There are two fundamental questions that arise from this discrepancy. First, “Does the geometry affect the star measurements?” and second, “Are the gravity measurements and local position vectors still collinear?”

The first question can be explored by first choosing a more realistic Earth model and investigating the actual geometric parameters associated with it. Two additional Earth models are the ellipsoid and the geoid. The ellipsoid model is more realistic than the spherical model because it accounts for the Earth’s equatorial bulge. The geoid model is the most accurate model and was constructed based upon local gravity measurements and digital elevation data. Whereas the geoid representation is closest to the physical geometry of the Earth, the ellipsoid (specifically, the World Geodetic System 1984 (WGS84) ellipsoid) is still appropriate for this research. The geoid model of the Earth would be very difficult to integrate into the stellar positioning system, especially since the system is intended to be deployed extra-terrestrially, where the extensive gravitational measurements needed may not be available.

The WGS84 Ellipsoid is identified as being a geocentric equipotential ellipsoid of revolution.⁵ An equipotential ellipsoid is simply an ellipsoid defined to be an equipotential surface, i.e., a surface on which the value of the gravity potential is the same everywhere. The WGS84 ellipsoid was generated using a combination of measurements including satellite radar altimetry, Doppler, satellite laser ranging, VLBI measurements, etc.

The use of the ellipsoid model gives rise to two distinct latitude angles as shown in figure 7. The geocentric latitude, ϕ_2 , is the angle between the equatorial plane and the line connecting the observer’s position and the Earth’s center. The geodetic latitude, ϕ_1 , is the angle between the equatorial plane and the line perpendicular to the ellipsoid at the observer’s position.

Due to the gravity gradient, the local gravity direction is perpendicular to the Earth’s equipotential surface. This means that plumb bobs and gravity gradient instruments will report the geodetic zenith as the local zenith direction. Although figure 7 exaggerates the Earth’s equatorial bulge and the gravity gradient effect, it is clear that the geodetic zenith and the geocentric zenith directions are different. How then, can the local position be accurately determined if no knowledge of the geocentric zenith direction exists? The answer to this question has two parts. First, the geodetic latitude must be converted to a corresponding geocentric latitude. Several convenient methods exist for performing the geodetic to geocentric conversion. One simple conversion formula, given in terms of the angles defined in figure 7, is the following.

$$\tan \phi_2 = \frac{r_p^2}{r_e^2} \tan \phi_1 \quad (21)$$

Here, r_p is the polar radius, 6,356.752 km, and r_e is the equatorial radius, 6,378.137 km. Secondly, the distance offset between the two observation vectors is inconsequential. That is, the error introduced by the geodetic latitude measurement is much smaller than the typical error magnitude of a star camera and can be considered negligible. This implies that two star images taken along parallel observation vectors but whose observation locations are separated by a given distance will show the same star field. The following discussion validates this point.

In order to analyze the worst-case scenario, the geodetic latitude is chosen to correspond to the maximum orthogonal distance, d , between the observation vectors (See figure 7). When $\phi_1 = 45^\circ$, $\phi_2 = 44.8076^\circ$ (Eq. 21), the magnitude of the geocentric radius is 6.367×10^6 km and d is 21313 km.

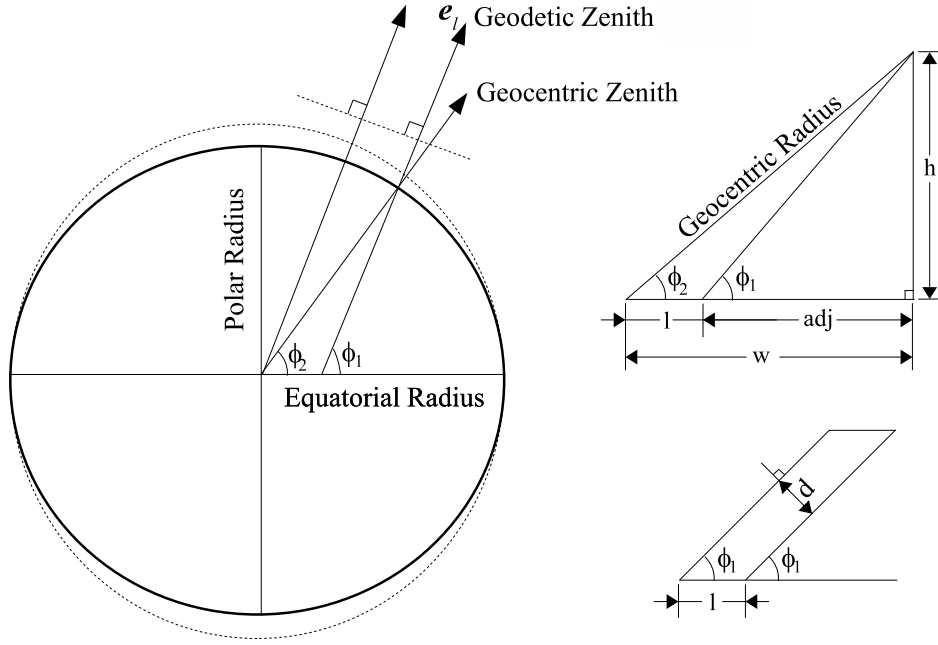


Figure 7. Geodetic and geocentric latitude angles.

The orthogonal distance, d , may be analytically determined as follows.

$$h = \sin \phi_2 |\mathbf{r}_{geocentric}| \quad (22a)$$

$$w = \cos \phi_2 |\mathbf{r}_{geocentric}| = l + \frac{h}{\tan \phi_1} \quad (22b)$$

$$l = \cos \phi_2 |\mathbf{r}_{geocentric}| - \frac{\sin \phi_2 |\mathbf{r}_{geocentric}|}{\tan \phi_1} \quad (22c)$$

$$d = l \sin \phi_2 \quad (22d)$$

The relationship between the observation vector angles and the geocentric latitude is shown in figure 8. Using Eq. 22 and the distance to the nearest star outside our solar system (α -Centauri, 4 light years), the largest angular separation of the vector observations is approximately 10^{-4} arcseconds. Therefore, the error introduced by the geodetic latitude measurement is much smaller than the typical error magnitude of a star camera and can be considered negligible.

The second question requires further exploration of the gravity vector. Magnitude is not of concern, but rather if one can truly equate the direction of local position vector, \mathbf{l} , to the local gravity vector, $-\mathbf{g}$, as explicitly assumed in the Vector Method. Using the standard parameters for terrestrial navigation, geodetic latitude (ϕ_1) and longitude (λ), the position vector relative to the Earth center in the ECEF frame $\{G\}$ is the following.⁶

$${}^G\mathbf{r} = \begin{bmatrix} \frac{r_e}{\sqrt{1-e^2 \sin^2 \phi_1}} \cos \phi_1 \cos \lambda \\ \frac{r_e}{\sqrt{1-e^2 \sin^2 \phi_1}} \cos \phi_1 \sin \lambda \\ \frac{r_e}{\sqrt{1-e^2 \sin^2 \phi_1}} (1-e^2) \sin \phi_1 \end{bmatrix} \quad (23)$$

Here, $e = \sqrt{1 - r_p^2/r_e^2} = 0.0818191908425$ is the eccentricity of an ellipsoidal model of the Earth, also from the 1984 World Geodetic System (WGS-84) standards. Recall that the geodetic latitude is defined with the assumption that the local position vector is perpendicular to this ellipsoidal model surface. Because ${}^G\mathbf{r}$

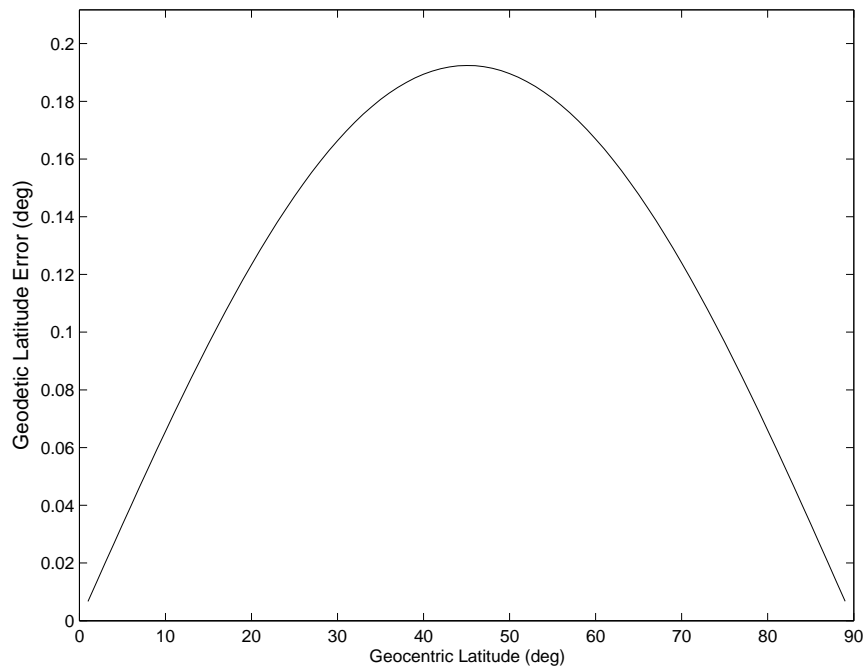


Figure 8. Geodetic / geocentric latitude comparison

is measured relative to the Earth's center, additional geometry must be used to convert this to the local position vector.

$${}^G\mathbf{l} = \begin{bmatrix} z \cos \lambda / \tan \phi_1 \\ z \sin \lambda / \tan \phi_1 \\ z \end{bmatrix} \Rightarrow \mathbf{e}_l = \begin{bmatrix} \cos \lambda \cos \phi_1 \\ \sin \lambda \cos \phi_1 \\ \sin \phi_1 \end{bmatrix} \quad (24)$$

Here, $z = {}^G\mathbf{r}(3)$ and \mathbf{e}_l is a the normalized (unit) vector related to ${}^G\mathbf{r}$. This local position vector is aligned with the Geodetic Zenith shown in figure 7.

Existing texts shed additional light on the question. In Groves, the gravity vector is implicitly related to the local position vector with the following statement.⁶

“The gravity vector at any point on the Earth's surface is perpendicular to the geoid, not the ellipsoid or the terrain, though, in practice, the difference is small.”

Furthermore, Groves later states:

“...the acceleration due to gravity is obtained from the gradient of the gravity potential, so it is not constant across the geoid. Although the true gravity vector is perpendicular to the geoid (not the terrain), it is a reasonable approximation for most navigation applications to treat it as perpendicular to the ellipsoid.”

Hofmann-wellenhof and Moritz note the following.

“...the deviations of the actual gravity field from the ellipsoidal ‘normal’ field are so small that they can be considered linear. This splitting of the earth's gravity field into a ‘normal’ and a remaining small ‘disturbing’ field considerably simplifies the problem of its determination; the problem could hardly be solved otherwise.”

(Here, gravity disturbances are related to, but conceptually different from, gravity anomalies.)

Complications with use of the geoid model have been previously discussed, but the distinction between the *gravity field* and the *gravitation field* can be further examined. The gravity vector can be decomposed

into two contributing components, the gravitational acceleration, $\boldsymbol{\gamma}$, and the acceleration due to the Earth's rotation.^{6,7} Note that the gravity vector is the specific force that is sensed by instruments.

$$\mathbf{g} = \boldsymbol{\gamma} - \boldsymbol{\omega}_e \times (\boldsymbol{\omega}_e \times \mathbf{r}) \quad (25)$$

The total acceleration due to gravity can be approximated from WGS-84 data using the Somigliana model.⁶ Note that a more rigorous derivation of a similar expression for this model is available in Hofmann-Wellenhof and Moritz.⁷

$$g_0(\phi_1) \approx 9.7803253359 \frac{1 + 0.001931853 \sin^2 \phi_1}{\sqrt{1 - e^2 \sin^2 \phi_1}} \quad (26)$$

Assuming that the gravity vector is perpendicular to the ellipsoidal surface, it can be further approximated.

$$\mathbf{g} \approx g_0(\phi_1) \mathbf{e}_l \quad (27)$$

This approximation appears to equate the geodetic latitude described in Groves with the astronomical latitude defined in Hofmann-Wellenhof and Moritz.^{6,7} The gravitational acceleration can be found by subtracting the acceleration due to the Earth's rotation.

$$\boldsymbol{\gamma} = \mathbf{g} + \boldsymbol{\omega}_e \times (\boldsymbol{\omega}_e \times \mathbf{r}) \quad (28)$$

Note that these results assume the position is on the equipotential surface, but can be modified for elevation above this surface by applying a simple scaling law.⁶ Here, the gravitational acceleration is derived using assumptions and measurements related to the gravity vector. However, we desire an independent calculation of the gravitational acceleration, which can be found when working in the ECI (inertial) reference frame.

$${}^I\boldsymbol{\gamma} = -\frac{\mu}{|{}^I\mathbf{r}|} \begin{bmatrix} \left[1 - 5 \left({}^I z / |{}^I\mathbf{r}|\right)^2\right] {}^I x \\ \left[1 - 5 \left({}^I z / |{}^I\mathbf{r}|\right)^2\right] {}^I y \\ \left[3 - 5 \left({}^I z / |{}^I\mathbf{r}|\right)^2\right] {}^I z \end{bmatrix} \quad (29)$$

Here, $\mu = 3.986004418 \times 10^{14} m^3 s^{-2}$ and ${}^I\mathbf{r} = ({}^I x, {}^I y, {}^I z) = \mathbf{R}_{I/G} {}^G\mathbf{r}$, with the following direction cosine matrix.

$$\mathbf{R}_{I/G} = \begin{bmatrix} \cos(\omega_e t) & -\sin(\omega_e t) & 0 \\ \sin(\omega_e t) & \cos(\omega_e t) & 0 \\ 0 & 0 & 1 \end{bmatrix} \quad (30)$$

Here, t is the elapsed time since t_0 . This rotation matrix, too, is a simplification of the transformation between the ECI (inertial) frame ECEF (Greenwich) frame.

The gravity vector calculated using the Somigliana model can then be compared to one constructed using the components of gravitational acceleration and acceleration due to the Earth's rotation. First, it is assumed that rotation about the Earth's spin axis is negligible such that $t = 0$ and $\lambda = 0$. Next, sweeping between the extreme values of geodetic latitude, $-\pi/2 \leq \phi_1 \leq \pi/2$, the gravity vector can be calculated using Eq. (26) as a first approximation and Eq. (29) with Eq. (25) as a second approximation. These vectors can then be compared to the normalized local position vector, \mathbf{e}_l , using $\triangle\theta = \arccos(\mathbf{g} \cdot \mathbf{e}_l)$ where θ is the angular error between the two vectors. Approximation 1 gives no new information, as it is defined in terms of \mathbf{e}_l . The results for Approximation 2, expressed in terms of the absolute value of the error, are shown in figure 9.

The maximum angular error shown is 1.3 arcseconds, which, when multiplied by the equatorial radius, translates to approximately 40.40 m. Given this order of error, it seems reasonable to conclude that the assumption of $\mathbf{e}_l = -\mathbf{g}/|\mathbf{g}|$ is valid with respect to the current level of accuracy achieved.² This approximation may be sufficient for SPS validation on Earth, but a full investigation and development of a gravity model will be necessary for extraterrestrial deployment. Additional considerations will include large local gravity perturbations, such as those from mascons on the moon, and third body effects, such as those from Earth or the sun.

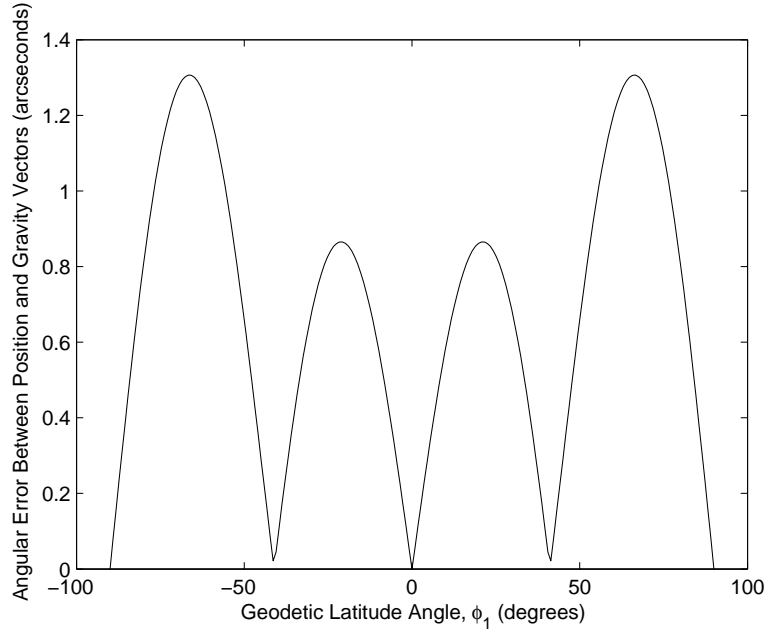


Figure 9. Angular Error between Gravity Vector Approximation 2 and Local Position Vector.

1. Ellipsoidal Earth Model Implications: Vector Method

The effect of an ellipsoidal Earth model on the measurements has been explored, but its manifestation in the vector method is also of interest. Consider a point on the Earth surface identified by the following geocentric vector.

$$\ell = \begin{Bmatrix} x_s \\ y_s \\ z_s \end{Bmatrix} = \mathbf{A} \begin{Bmatrix} \cos \phi_2 \cos \lambda \\ \cos \phi_2 \sin \lambda \\ \sin \phi_2 \end{Bmatrix} \quad (31)$$

where the angle ϕ_2 is still the *geocentric* latitude and $\mathbf{A} = \mathbf{A}(\phi_2)$ the unknown geocentric radius vector. This point belongs to an axial-symmetric ellipsoidal surface if it satisfies the following equation.

$$\frac{x_s^2 + y_s^2}{r_e^2} + \frac{z_s^2}{r_p^2} = 1 \quad (32)$$

The equation of a plane tangent to the ellipsoid at point ℓ is then as follows.

$$\frac{x x_s + y y_s}{r_e^2} + \frac{z z_s}{r_p^2} = 1 \quad (33)$$

The vector normal to the plane given by Eq. (33) is aligned with the local gravity direction.

$$\ell' = \begin{Bmatrix} x_s/r_e^2 \\ y_s/r_e^2 \\ z_s/r_p^2 \end{Bmatrix} = \mathbf{A}' \begin{Bmatrix} \cos \phi_1 \cos \lambda \\ \cos \phi_1 \sin \lambda \\ \sin \phi_1 \end{Bmatrix} = \frac{\mathbf{A}}{r_e^2} \begin{Bmatrix} \cos \phi_2 \cos \lambda \\ \cos \phi_2 \sin \lambda \\ (1-f)^{-2} \sin \phi_2 \end{Bmatrix} \quad (34)$$

Here, recall that ϕ_1 is the *geodetic* latitude and $\mathbf{A}' = \mathbf{A}'(\phi_1)$ the unknown geodetic radius vector.

Equation (8) states that the angle between stars and the local gravity direction is independent from reference frame. This property does not change if the gravity direction points to a point other than the Earth center (e.g., aligned toward the geodetic direction). Therefore, if \mathbf{g} is aligned with the geodetic direction, then ℓ' will also point along the same direction. Therefore, the identical solution given by Eq.

(10), also applies to this Earth model.

$$\ell' = -(\mathbf{A}_g^T \mathbf{A}_g)^{-1} \mathbf{A}_g^T \mathbf{A}_c \mathbf{g} = \begin{Bmatrix} \cos \phi_1 \cos \lambda \\ \cos \phi_1 \sin \lambda \\ \sin \phi_1 \end{Bmatrix} \quad (35)$$

The only difference here is that $\ell' = \mathbf{e}_l$ indicates the *geodetic* direction, the location provided by a GPS receiver.

B. Earth-Centered Earth-Fixed Reference Frame

The construction of $\mathbf{R}_{G/I}$ attitude matrix can be very complex. This consequence arises from the influence by a number of physical factors, some of which occur over long time spans and others that are neither completely understood nor predictable. Two effects that are relatively well understood, precession and nutation, will be described, as well as the Greenwich angle, ψ (see figure 1). The polar motion, less well understood, deals with deviations from the predicted motion of Earth and can be calculated using the Earth Orientation Parameters (EOPs). Accounting for the combination of these effects will allow for the final construction of $\mathbf{R}_{G/I}$.

Two separate $\mathbf{R}_{G/I}$ prediction models will be presented in this section, the Vallado model⁸ and the IERS 2000 model.⁹ The $\mathbf{R}_{G/I}$ prediction models differ mainly in their treatment of the nutation and precession matrix. The slight numerical differences between the models in the Greenwich angle calculation and the polar motion correction will not be examined here.

One well-established principal of celestial mechanics is that the attitude of the Earth with respect to the ecliptic plane changes with time. One of the dominant motions affecting this change in attitude is the precession of the Earth's spin axis. This motion is caused by gravity torques produced by the Moon and Sun. Due to this precession, the Earth's spin axis sweeps out a 23.45° half-angle cone every 26000 years. In addition to the precession of the Earth's spin axis, the ecliptic poles move with respect to time although much more slowly than the spin axis precession. The combined effect of these two motions is called general precession.

The predictable short-term deviation of the Earth's spin axis from its long term precession is called nutation. The nutation transformation is required to account for the periodic effects the Moon and Sun have on the Earth. Nutational effects have a period of roughly 19 years and a maximum displacement angle of 0.005° .

The nutation and precession component of the Vallado model can be written as the product of four Euler rotation matrices as follows.

$$NP = \mathbf{R}_1(-\alpha) \mathbf{R}_3(-\beta) \mathbf{R}_1(\gamma) \mathbf{R}_3(\delta) \quad (36)$$

The angles γ and δ are the angles that specify the location of the ecliptic pole in the given inertial frame, β is the ecliptic angle of precession, and α is the obliquity of the ecliptic. All of these angles are functions of the current time and may be solved using the following set of equations.

$$\begin{aligned} \alpha &= (84381.4428 - 46.8388t - 0.0002t^2 + 0.002t^3)/3600 \\ \beta &= (-0.0431 + 5038.4739t + 1.5584t^2 - 0.0002t^3)/3600 \\ \gamma &= (84381.4479 - 46.814t + .0511t^2 + .0005t^3)/3600 \\ \delta &= (10.5525t + 0.4932t^2 - 0.0003t^3)/3600 \end{aligned} \quad (37)$$

Here, the current time, t , is found using the current Julian Date, JD , the J2000 Julian Date, ($T_0 = 2451545$), and the number of days in one century, ($T_{century} = 36525$).

$$t = (JD - T_0)/T_{century} \quad (38)$$

The IERS 2000 model then calculates the nutation and precession matrix as the following.

$$NP = \mathbf{R}_3(-E) \mathbf{R}_2(-d) \mathbf{R}_3(E) \mathbf{R}_3(s) \quad (39)$$

Here, E and d correspond to the location of the celestial intermediate pole in the celestial reference system using the following transformation.

$$X = \sin d \cos E, \quad Y = \sin d \sin E, \quad Z = \cos d \quad (40)$$

The term, s , can be expressed in terms of X and Y using the following equation.

$$s(t) = - \int_{t_0}^t \frac{X(t)\dot{Y}(t) - Y(t)\dot{X}(t)}{1 + Z(t)} dt - (\sigma_0 N_0 - \Sigma_0 N_0) \quad (41)$$

Here, σ_0 , Σ_0 , and N_0 are coordinates of the celestial ephemeris origin and the ascending node of the equator at J2000. A full development and more detailed description of the variables is available in Ref. 9. For the purposes of this research, the nutation and precession matrix was calculated directly from the X and Y variables using the following equation.

$$NP(t) = \begin{pmatrix} 1 - aX^2 & -aXY & X \\ -aXY & 1 - aY^2 & Y \\ -X & -Y & 1 - a(X^2 + Y^2) \end{pmatrix} \cdot \mathbf{R}_3(s) \quad (42)$$

Here, a is formally defined as $a = 1/(1 + \cos d)$, but in order to simplify the calculation, a was approximated as $a = 1/2 + 1/8(X^2 + Y^2)$.

Another component of the $\mathbf{R}_{G/I}$ calculation is the determination of the Greenwich meridian angle. This angle is also referred to as the Earth rotation angle. The angle, ψ , can be written as an explicit function of time.

$$\psi(T_u) = 2\pi(0.779057273264 + 1.00273781191135448T_u). \quad (43)$$

Here, T_u is amount of Julian time since J2000 using the IERS UT1-UTC correction.

The final component of the $\mathbf{R}_{G/I}$ is the polar motion correction. In order to generate the most accurate local position coordinates, several factors must be considered in addition to general precession and nutation to properly calculate the Earth's orientation. These additional factors are natural forces that have a weaker effect than precession and nutation and therefore are a means to fine tune the local position calculation. For example, the Chandler Wobble is an effect that is often attributed to the thermal currents in the Earth's oceans. Although hypotheses exist to describe the various natural forces that affect $\mathbf{R}_{G/I}$, a long-term model capable of predicting the effects does not exist. Until such a predictive model exists, accounting for effects from natural forces' will require adjustments made possible by scientific observations. The observation data is publicly released by the USNO and the IERS. These institutions also publish short-term prediction bulletins. Therefore, realtime local position determination must rely on a direct link to the EOP reporting services or the USNO EOP predictions. The general equation used to account for polar motion is the following.

$$W(t) = \mathbf{R}_3(-s')\mathbf{R}_2(x_p)\mathbf{R}_1(y_p) \quad (44)$$

Here, x_p , y_p , and s' are the polar coordinates of the celestial intermediate pole in the terrestrial reference system and the position of the terrestrial ephemeris origin on the equator of the celestial intermediate pole, respectively. The x_p and y_p values are fully defined by summing the IERS reported values and two additional terms that address effects with periods less than two days as follows.

$$(x_p, y_p) = (x, y)_{IERS} + (\Delta x, \Delta y)_{tidal} + (\Delta x, \Delta y)_{nutation} \quad (45)$$

For the purposes of this research, the (x_p, y_p) quantities were assumed to be equivalent to the IERS reported (x, y) values. The s' term was calculated using the following approximation.

$$s' = -47t \mu\text{as} \quad (46)$$

Here, t is found using Eq. 38 and μas is the unit, micro-arcseconds.

The nutation and precession, Earth rotation angle, and polar motion offset matrices are combined to generate the $\mathbf{R}_{G/I}$ attitude matrix according to the following equation.

$$\mathbf{R}_{G/I}(t) = NP(t)\mathbf{R}_3(-\psi(T_u))W(t) \quad (47)$$

The Vallado and IERS 2000 models both make use of Eq. 47 with the primary difference in the resulting $\mathbf{R}_{G/I}$ due to the alternate nutation and precession models. It should be noted that several approximations and assumptions were made in order to simplify the IERS 2000 $\mathbf{R}_{G/I}$ calculations presented in this section. To further increase the accuracy of the $\mathbf{R}_{G/I}$ matrix, and therefore the position determination results, the full series expansions and complete predictions of the IERS 2000 model would need to be implemented.

While these two models provide greater accuracy for an Earth-based positioning system, the SPS is intended to be an autonomous system. That is, as an autonomous system, the SPS would not have access to the regularly published parameters necessary to implement the IERS nutation-precession model and calculate the polar motion for both models. If the small effect of polar motion is neglected, the Vallado model can be implemented. Furthermore, since the nutation-precession matrix is also close to identity, a variation of the Greenwich angle called the apparent Greenwich sidereal time, can be used with a simple rotation about the Earth axis. This version of the Greenwich angle takes into account a lower order approximation of the nutation angle using the first few terms of the IAU 1980 nutation algorithm. This simpler choice for the ECEF attitude transformation matrix is more readily translated for use on extraterrestrial bodies, given a low-order approximation of the body's "Greenwich" angle.

VI. Conclusions

Of the two position determination algorithms, the vector method is the most straight-forward and therefore least error-prone. Consequently, its implementation will be the focus of future work. Still, implementation of either algorithm in hardware is far more complicated than the underlying ideas. Hardware limitations and error sources, such as image quality, field of view, and measurement precision must be overcome via significant efforts in calibration, filtering, and error modeling. Initial error source analysis indicates that time precision, and its subsequent effect on the Greenwich reference frame calculation, may have the greatest effect on accuracy after successful hardware calibration. Still, with minimal system calibration and image post-processing, preliminary experiments have yielded position estimates to within 2 km. Additional error mitigation techniques, as presented in Stellar Positioning System (Part II), reduce this error to 50 m. Future extraterrestrial models and hardware development will move the SPS toward a viable autonomous position determination solution on the moon and Mars.

References

- ¹Herman, L., "The History, Definition and Peculiarities of the Earth Centered Inertial (ECI) Coordinate Frame and the Scales that Measure Time," *Proceedings of the IEEE Aerospace Applications Conference*, Vol. 2, February 1995, pp. 233–263.
- ²Woodbury, D., Parish, J., Parish, A., Swanzy, M., Denton, R., Mortari, D., and Junkins, J. L., "Stellar Positioning System (Part II): Overcoming Error During Implementation," *AIAA Guidance, Navigation, and Control Conference*, 18–21 August 2008, Honolulu, Hawaii.
- ³Mortari, D., Samaan, M. A., Bruccoleri, C., and Junkins, J. L., "The Pyramid Star Identification Technique," *Navigation*, Vol. 51, No. 3, Fall 2004, pp. 171–183.
- ⁴Mortari, D., "Second Estimator of the Optimal Quaternion," *Journal of Guidance, Control, and Dynamics*, Vol. 23, No. 5, September–October 2000, pp. 885–888.
- ⁵Mularie, W., "Department of Defense World Geodetic System 1984: Its Definition and Relationships with Local Geodetic Systems," Tech. rep., National Imagery and Mapping Agency, January 2000.
- ⁶Groves, P. D., *Principles of GNSS, Inertial, and Multisensor Navigation Systems*, Artech House, Boston, MA, 2008.
- ⁷Hofmann-Wellenhof, B. and Moritz, H., *Physical Geodesy*, SpringerWienNewYork, Vöslau, Austria, 2005.
- ⁸Vallado, D. A., *Foundations of Astrodynamics and Applications*, Kluwer Academic Publishers, El Segundo, California, 2nd ed., 2001.
- ⁹McCarthy, D. and Petit, G., "IERS Conventions (2003)," Tech. rep., International Earth Rotation and Reference Systems Service, Frankfurt, Germany, 2004.